Validation and application of optimal ionospheric shell height model for single-site TEC estimation

Jiaqi Zhao[1], Chen Zhou[1]

School of Electronic Information, Wuhan University, Wuhan, 430072, China

Corresponding to: chenzhou@whu.edu.cn

Abstract

We recently proposed a method to establish optimal ionospheric shell height model based on the international GNSS service (IGS) station data and the differential code bias (DCB) provided by Center for Orbit Determination in Europe (CODE) during the time from 2003 to 2013. This method is very promising for DCB and accurate total electron content (TEC) estimation by comparing to traditional fixed shell height method. However, this method is basically feasible only for IGS stations. In this study, we investigate how to apply the optimal ionospheric shell height derived from IGS station to non-IGS stations or isolated GNSS receivers. The intuitional and practical method to estimate TEC of non-IGS stations is based on optimal ionospheric shell height derived from nearby IGS stations. To validate this method, we selected two dense networks of IGS stations located in US and Europe region. Two optimal ionospheric shell height models are established by two reference stations, namely GOLD and PTBB, which are located at the approximate center of two selected regions. The predicted daily optimal ionospheric shell heights by the two models are

applied to other IGS stations around these two reference stations. Daily DCBs are calculated according to these two optimal shell heights and compared to respective DCBs released by CODE. The validation results of this method present that 1) Optimal ionospheric shell height calculated by IGS stations can be applied to its nearby non-IGS stations or isolated GNSS receivers for accurate TEC estimation. 2) As the distance away from the reference IGS station becomes larger, the DCB estimation error becomes larger. The relation between the DCB estimation error and the distance is generally linear.

Keyword

Ionospheric shell height, Single layer model (SLM), Differential code bias (DCB), Total electron content (TEC)

Introduction

Dual-frequency GPS signals propagation are affected effectively by ionospheric dispersive characteristic. While, by taking advantage of this property, ionospheric TEC along the path of signal can be estimated by using differencing the pseudorange or carrier phase observations from dual-frequency GPS signals. Carrier phase leveling/smoothing of code measurement is widely adopted to improve the precision of absolute TEC observations (Mannucci et al. 1998; Horvath and Crozier 2007). In

42 general, it is considered that the derived TEC in carrier phase leveling/smoothing
43 technique consists of slant TEC (STEC), the combination differential code bias (DCB)
44 of satellite and receiver, multipath effects and noise. The DCB is usually considered
45 as the main error source and could be as large as several TECu (Lanyi and Roth 1988;
46 Warnant 1997).

47 For TEC and DCB estimations, mapping function with single layer model (SLM)
48 assumption have been intensively studied for many years. Sovers and Fanselow (1987)
49 firstly simplified the ionosphere to a spherical shell. They set the bottom and the top
50 side of the ionospheric shell as h-35 and h+75 km, where h is taken to be 350 km
51 above the surface of the earth and allowed to be adjusted. In this model, the electron
52 density was evenly distributed in the vertical direction. Based on this model, Sardón et
53 al. (1994) introduced the Kalman filter method for real-time ionospheric VTEC
54 estimation. Klobuchar (1987) assumed that STEC equals VTEC multiplied by the
55 approximation of the standard geometric mapping function at the mean vertical height
56 of 350 km along the path of STEC. Lanyi and Roth (1988) further developed this
57 model into a single thin-layer model, and proposed the standard geometric mapping
58 function and the polynomial model. The single thin-layer model assumed that the
59 ionosphere is simplified by a spherical thin shell with infinitesimal thickness. Clynch
60 et al (1989) proposed a mapping function in the form of a polynomial by assuming a
61 homogeneous electron density shell between altitudes of 200 and 600 km. Mannucci
62 et al (1998) presented an elevation scaling mapping function derived from extended

63 slab mode. There are also many modified mapping function according to the standard
64 geometric mapping function. Schaer (1999) proposed the modified standard mapping
65 function using a reduced zenith angle. Rideout and Coster (2006) presented a new
66 mapping function which replaces the influence of the shell height by an adjustment
67 parameter, and set the shell height as 450 km. Smith et al (2008) modified the
68 standard mapping function by using a complex factor. Based on the electron density
69 field derived from the international reference ionosphere (IRI), Zus et al (2017)
70 recently developed an ionospheric mapping function at fixed height of 450 km with
71 dependence on time, location, azimuth angle, elevation angle, and different
72 frequencies.

73 Ionospheric shell height is considered to be the most important parameter for
74 mapping function, and the shell height is typically set to a fixed value between 350
75 and 450 km (Lanyi and Roth 1988; Mannucci et al. 1998). Birch et al. (2002)
76 proposed an inverse method for estimate the shell height by using simultaneous
77 VTEC and STEC observations, and suggested the shell height is preferred to be a
78 value between 600 and 1200 km. Nava et al. (2007) presented a shell height
79 estimation method by minimizing the mapping function errors, this method is referred
80 as the “coinciding pierce point” technique. Their results indicated that the suitable
81 shell heights for the mid-latitude is 400 km and 500 km during the geomagnetic
82 undisturbed conditions and disturbed conditions, respectively. In the case of the
83 low-latitude, the shell height at about 400 km is suitable for both quiet and disturbed

84 geomagnetic conditions. Jiang et al. (2018) applied this technique to estimate the
85 optimal shell height for different latitude bands. In their case, the optimal layer height
86 is about 350 km for the entire globe. Brunini et al. (2011) studied the influence of the
87 shell height by using an empirical model of the ionosphere, and pointed out that a
88 unique shell height for whole region does not exist. Li et al. (2017) applied a new
89 determination method of the shell height based on the combined IGS GIMs and the
90 two methods mentioned above to the Chinese region, and indicated that the optimal
91 shell height in China ranges from 450 to 550 km. Wang et al. (2016) studied the shell
92 height for grid-based algorithm by analyzing goodness of fit for STEC. Lu et al. (2017)
93 applied this method to different VTEC models, and investigated the optimal shell
94 heights at solar maximum and at solar minimum.

95 In the recent study by Zhao and Zhou (2018), a method to establish optimal
96 ionospheric shell height model for single station VTEC estimation has been proposed.
97 This method calculates the optimal ionospheric shell height with regards to minimize
98 |ΔDCB| by comparing to the DCB released by CODE. Five optimal ionospheric shell
99 height models were established by the proposed method based on the data of five IGS
100 stations at different latitudes and the corresponding DCBs provided by CODE during
101 the time 2003 to 2013. For the five selected IGS stations, the results have shown that
102 the optimal ionospheric shell height models improve the accuracies of DCB and TEC
103 estimation comparing to fixed ionospheric shell height of 400 km in a statistical sense.
104 We also found that the optimal ionospheric shell height show 11-year and 1-year

periods and is related to the solar activity, which indicated the connection of the optimal shell height with ionospheric physics.

While the proposed optimal ionospheric shell height model is promising for DCB and TEC estimation, this method cannot be implemented to isolated GNSS receivers not belonging to IGS stations. The purpose of this study is to investigate the application of the optimal ionospheric shell height derived from IGS station to non-IGS stations. By considering the spatial correlation of ionospheric electron density, it is intuitional and practical to adopt the optimal ionospheric shell height of a nearby IGS station for the non-IGS stations.

The purpose of this study is to investigate the feasibility of applying the optimal ionospheric shell height derived from IGS station to nearby non-IGS GNSS receivers for accurate TEC/DCB estimation. By selecting two different regions in U.S. and Europe with dense IGS stations, we calculate the daily DCBs of 2014 by using the optimal ionospheric shell heights derived from 2003-2013 data of two central stations in two regions. We also try to find the DCB estimation error and its relation to distance away from the central reference station.

Method

In (Zhao and Zhou, 2018), we proposed a concept of optimal ionospheric shell height for accurate TEC and DCB estimation. Based on daily data of single site, this approach searches daily optimal ionospheric shell height, which minimizes the

difference between the DCBs calculated by VTEC model for single site and reference values of DCB. For a single site, its long-term daily optimal ionospheric shell heights can be estimated and then modeled. In our case, the polynomial model (Lanyi and Roth 1988; Wild 1994) is applied to estimate satellite and receiver DCBs, and the DCBs provided by CODE are used as the reference.

In the polynomial model, the VTEC is considered as a Taylor series expansion in latitude and solar hour angle, which is expressed as follows:

$$T_V(\varphi, S) = \sum_{i=0}^{m}\sum_{j=0}^{n} E_{ij}(\varphi - \varphi_0)^i (S - S_0)^j \quad (1)$$

where T_V denotes VTEC. φ and S denote the geographic latitude and the solar hour angle of ionospheric pierce point (IPP), respectively; φ_0 and S_0 denote φ and S at regional center. E_{ij} is the model coefficient. m and n denote the orders of the model. A polynomial model fits the VTEC over a period of time. In our case, 8 VTEC models are applied per day, and DCB is considered as constant in one day. Since our analysis is based on long-term single site data, we set *m* and *n* to 4 and 3, respectively. Huang and Yuan (2014) applied the polynomial model with the same orders to TEC estimation.

Based on the thin shell approximation, the observation equation can be written as:

$$T_{os}^{PRN}(\varphi, S) = T_V(\varphi, S) \cdot f(z) + DCB^{PRN} \quad (2)$$

where T_{os}^{PRN} is slant TEC calculated by carrier phase smoothing, the superscript *PRN* denotes GPS satellite. DCB^{PRN} denotes the combination of GPS satellite and

147 receiver DCB. *z* denotes the zenith angle of IPP. According to Lanyi and Roth (1988),
148 the standard geometric mapping function $f(z)$ is expressed as follows:

149 $$f(z) = 1/\cos(z) \tag{3}$$

150 $$z = \arcsin \frac{\mathrm{Re} \cdot \cos El}{\mathrm{Re} + h} \tag{4}$$

151 where Re denotes the earth's radius, El denotes the elevation angle, and *h* denotes
152 the thin ionospheric shell height. Note that *h* also affects the location of IPP.

153 To estimate DCBs, The method above requires a definite thin shell height value.
154 Conversely, if we get the daily solutions of DCBs, the optimal ionospheric shell
155 height can be estimated. The optimal ionospheric shell height is assumed to be
156 between 100 and 1000 km and is defined as the shell height with the minimum
157 difference between DCB^{PRN} and the reference values. This optimization problem can
158 be written as:

159 $$\min_{100<h<1000} mean\left(\left|\mathbf{DCB_{ref}} - \mathbf{DCB}\right|\right) \text{ s.t. } \mathbf{T} = \mathbf{\Phi} \cdot \mathbf{E} + \boldsymbol{\theta} \cdot \mathbf{DCB} \tag{5}$$

160 where h is the daily optimal ionospheric shell height, $\mathbf{DCB_{ref}}$ denotes the vector of
161 the reference values of DCBs, s.t. is the abbreviation for subject to,
162 $\mathbf{T} = \mathbf{\Phi} \cdot \mathbf{E} + \boldsymbol{\theta} \cdot \mathbf{DCB}$ is the matrix form of all the observation equations in one day,
163 $\mathbf{T}$ denotes the vector of T_{os}, $\mathbf{E}$ corresponds to the coefficients of the models,
164 $\mathbf{DCB}$ is the vector of DCB^{PRN}, $\mathbf{\Phi}$ and $\boldsymbol{\theta}$ are the coefficient matrix of $\mathbf{E}$ and
165 $\mathbf{DCB}$, respectively.

166 After the method above is applied to 11-year data, the estimated optimal
167 ionospheric shell heights can be modeled by a Fourier series, which is expressed as

follows:

$$h(x) = a_0 + \sum_{n=1}^{k}\left(a_n \cos\frac{2n\pi x}{L} + b_n \sin\frac{2n\pi x}{L} \right) \quad (6)$$

where k is the order of Fourier series and is set to 40, a_n and b_n are the model coefficients, x is the time, and L is the time span which equals to 4018 days. The maximum frequency of model is 40/L≈0.01 per day. By least square method, the model coefficients can be estimated. The estimated daily optimal ionospheric shell height $h(x)$ by the model is then applied to other neighboring stations in this region. By using $h(x)$, we can validate the TEC and DCB estimation.

Experiment and Results

The previous section introduced a method to establish daily optimal ionospheric shell height model based on single site with reference values of DCBs. To analyze the improvement of DCB estimation by this model for the reference station and other neighboring stations, we present two experiments to evaluate and validate this method by using IGS stations located in U.S. and Europe region. To ensure the accuracy and consistency of DCB, we only select IGS stations with pseudorange measurements of P1 code, and whose receiver DCBs have been published by CODE.

Figure 1 presents the location and distribution of the selected IGS stations in two regions. Table 1 presents the information of the geographical location, distance to reference station in each region and receiver types of all stations. Based on the

RINEX data of GOLD station in Region I and PTBB station in Region II during the period of 2003-2013, two separate optimal ionospheric shell height models for each region are established by the aforementioned method. Then the model are applied to DCB estimation in 2014 for all the other stations in each region. Note that reference GOLD and PTBB stations are marked with black triangle in the figure. The other neighboring stations are located in different orientations of GOLD and PTBB with different distances, which range from 136 to 1159 km for region I and range from 190.82 to 1712.27 km for region II. In the table, the receiver type is corresponding to 2003~2014 for GOLD and PTBB, and 2014 for the other stations. In region I, the receiver type of GOLD have been changed once in September 2011. The five selected stations used four receiver types in 2014; TABV and PIE1 had the same receiver type. In region II, there are nine receiver types for the sixteen stations. The receiver type of PTBB have changed twice in 2006.

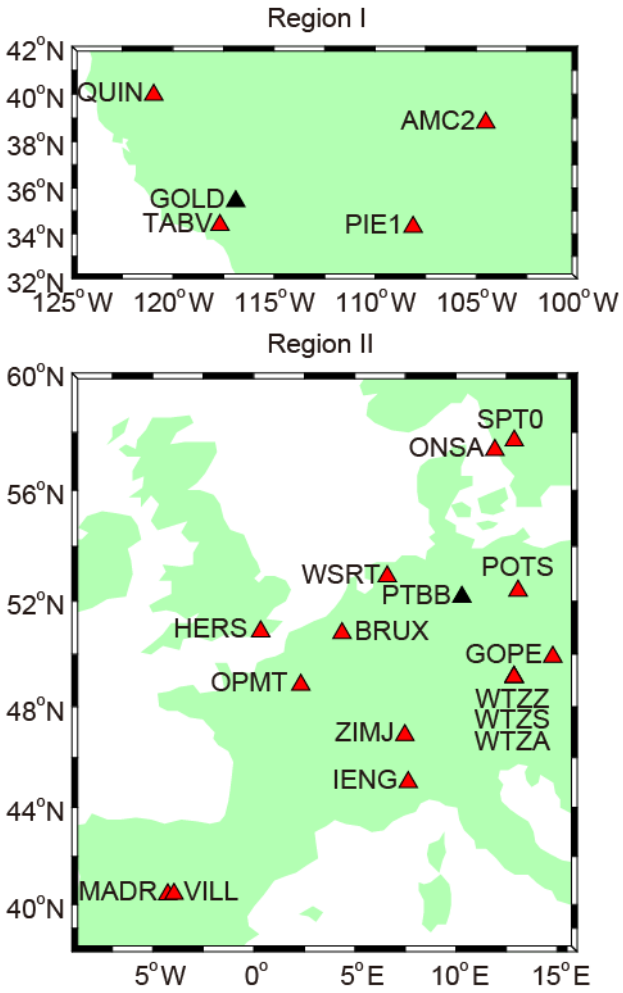

202

203 **Fig.1** Geographical location of the selected IGS stations in U.S. region (Region I) and

204 Europe region (Region II).

205

206

207 **Table 1** Information for the stations

Name	Latitude (deg)	Longitude (deg)	Distance to GOLD or PTBB (km)	Receiver type
GOLD	35.42	-116.89	0	ASHTECH Z-XII3 ~ 2011-09-14 JPS EGGDT 2011-09-19 ~
TABV	34.38	-117.68	136.67	JAVAD TRE_G3TH DELTA
QUIN	39.97	-120.94	619.55	ASHTECH UZ-12

PIE1	34.30	-108.12	810.51	JAVAD TRE_G3TH DELTA
AMC2	38.80	-104.52	1159.09	ASHTECH Z-XII3T
PTBB	52.15	10.30	0	SEPT POLARX2 2006-07-25~ 2006-11-13 ASHTECH Z-XII3T else
POTS	52.38	13.07	190.82	JAVAD TRE_G3TH DELTA
WSRT	52.91	6.60	264.92	AOA SNR-12 ACT
WTZA	49.14	12.88	381.28	ASHTECH Z-XII3T
WTZS	49.14	12.88	381.28	SEPT POLARX2
WTZZ	49.14	12.88	381.28	JAVAD TRE_G3TH DELTA
GOPE	49.91	14.79	401.51	TPS NETG3
BRUX	50.80	4.36	439.03	SEPT POLARX4TR
ONSA	57.40	11.93	593.72	JPS E_GGD
ZIMJ	46.88	7.47	620.79	JAVAD TRE_G3TH DELTA
SPT0	57.72	12.89	641.78	JAVAD TRE_G3TH DELTA
OPMT	48.84	2.33	674.24	ASHTECH Z-XII3T
HERS	50.87	0.34	705.38	SEPT POLARX3ETR
IENG	45.02	7.64	816.64	ASHTECH Z-XII3T
VILL	40.44	-3.95	1696.62	SEPT POLARX4
MADR	40.43	-4.25	1712.27	JAVAD TRE_G3TH DELTA

208

209 Figure 2 presents the estimated daily optimal ionospheric shell height of GOLD
210 and PTBB during the period from 2003 to 2013. The left panel shows the variation of
211 the daily optimal ionospheric shell height and the fitting result by (6). From the
212 overall trend, the variations of daily optimal ionospheric shell height for both two
213 stations appear wave-like oscillation during the 11 years period. In the right panel, the

statistical result are fitted by a normal distribution. The mean and the standard deviation (STD) of the normal distribution are 714.3 and 185.4 km for GOLD, respectively. The mean and STD value for PTBB is 416.4 and 184.1 km, respectively.

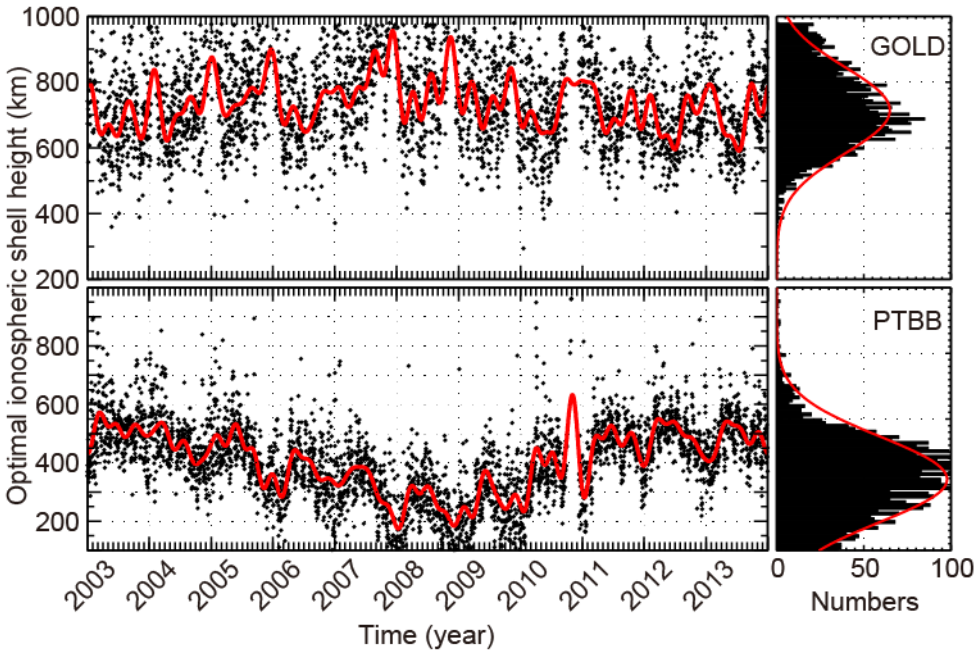

Fig.2 Variation of the daily optimal ionospheric shell height (black) and the fitting result (red)

Figure 3 presents the amplitude spectra of the daily optimal ionospheric shell height of two reference stations estimated by the Lomb-Scargle analysis (Lomb 1976; Scargle 1982). As can be found in Figure 3, the peaks correspond to 11-year, 1-year, 6-month and 4-month cycles. The amplitudes of 11-year and 1-year cycles are more evident than other periods in both two stations. Note that the frequencies above 0.01 per day are discarded because of their small amplitudes. As mentioned earlier, 0.01 per day is about the maximum frequency of (6). This result shows that the optimal

ionospheric shell height of GOLD and PTBB is periodic, and the 40th-order of Fourier series is suitable for modelling its variation.

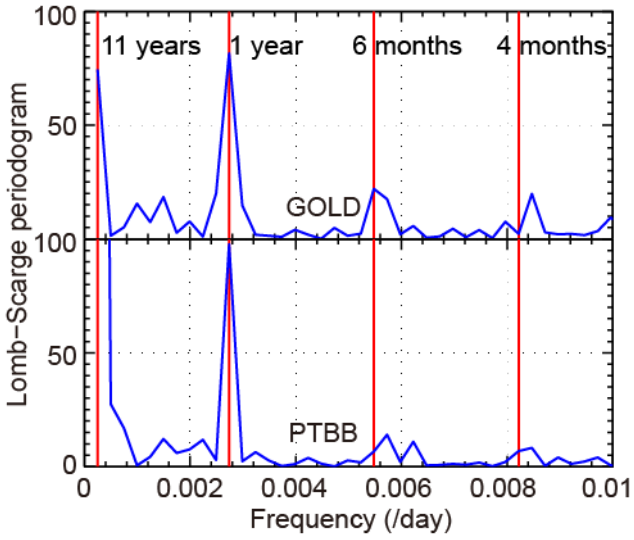

Fig.3 Lomb-Scargle spectra of the daily optimal ionospheric shell height

We establish two optimal ionospheric shell height models for each region by the 40th-order of Fourier series based on the 11-year data of GOLD and PTBB. To investigate the availability zone of the optimal ionospheric shell height model, we apply the model to the stations of each region as shown in Figure 1 and Table 1. Based on the predicted daily optimal ionospheric shell heights in 2014 calculated by the model of GOLD and PTBB, the DCBs in all stations of each region are estimated in the form of single station by the polynomial model mentioned earlier. The difference of DCBs in all station in each region calculated by the optimal ionospheric shell height model from each reference station and DCBs provided by CODE is then

compared to the difference of DCBs calculated by fixed ionospheric shell height (400 km) and DCBs released by CODE.

Figure 4 shows the daily average differences of DCBs calculated by the model and DCBs of each stations provided by CODE in 2014, and the differences of DCBs calculated by the fixed ionospheric shell height (400 km) and DCBs released by CODE in 2014. The panels for the stations are arranged by their distances to reference station, this is also applied to the following table; from the top panels to the bottom panels, the distance of the corresponding station to the reference station gradually increases. The left and right panels show the daily differences and the histograms of the statistical results in 2014, respectively. For all of the stations, the daily average differences of DCBs calculated by the optimal ionospheric shell height model are reduced compared to the fixed ionospheric shell height. For GOLD and TABV, the reductions are appropriate, the daily average ΔDCBs around 0 have the most days. For the other stations, the reductions are so much that most of the average ΔDCBs are negative. This result shows the improvement of the model seems to be related with the distance to GOLD. Note that some days no result because of missing data. Figure 5 is the same format as Figure 4, which presents the results of Region II. By comparing to the results of fixed ionospheric height, Figure 5 also indicates that the ΔDCB of optimal ionospheric shell heights with PTBB prediction is more concentrated distributed around 0 in a statistical sense. Both Figure 4 and Figure 5 present the accuracy of DCB estimation by using optimal ionospheric heights from reference

265 station, namely GOLD and PTBB in this study, can be improved.

266

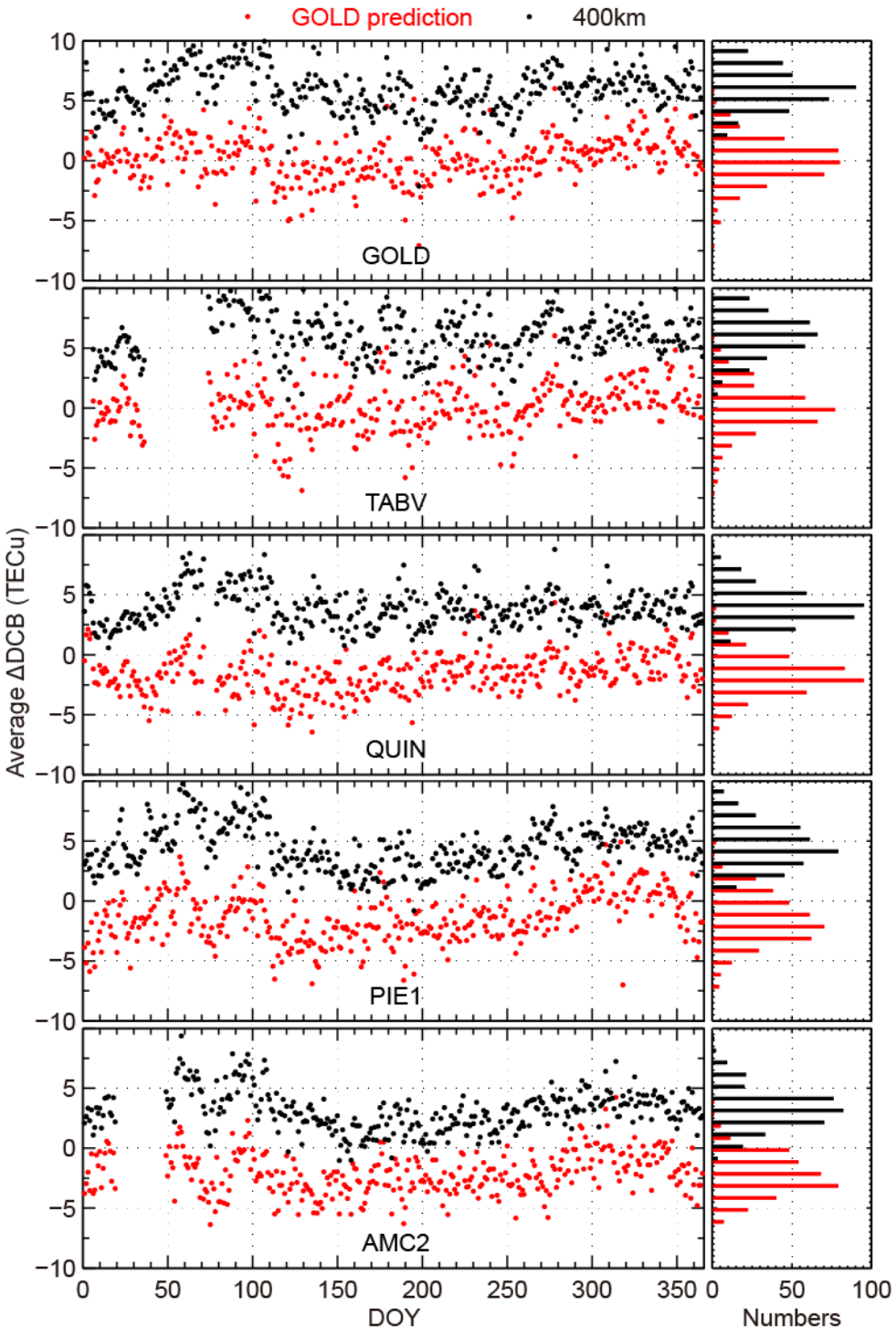

267

268 **Fig.4** Comparisons of the average ΔDCB calculated by the predicted optimal

269 ionospheric shell heights (red dots) and by the fixed ionospheric shell height (black

dots) in 2014 for stations in Region I.

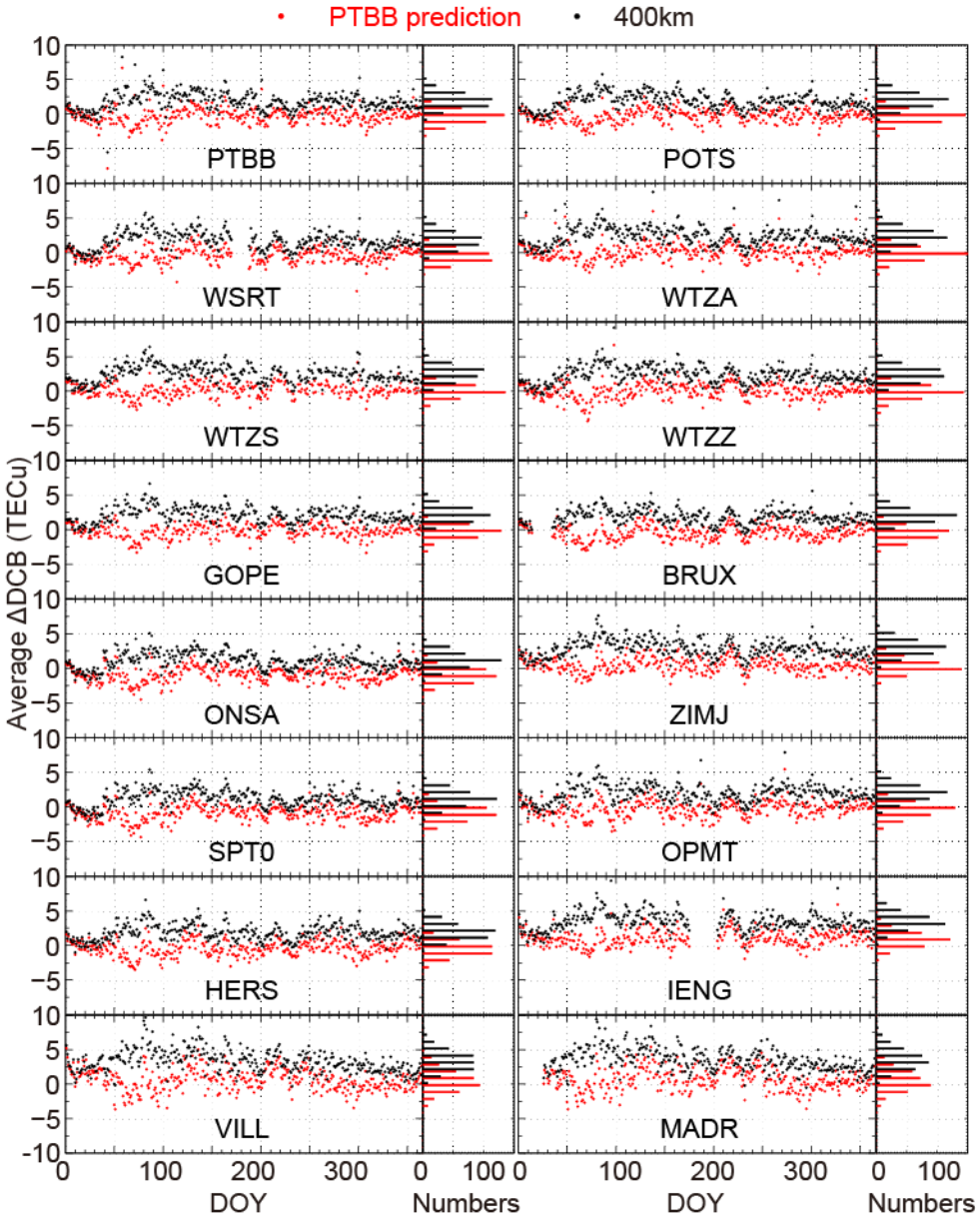

Fig.5 Comparisons of the average ΔDCB calculated by the predicted optimal ionospheric shell heights (red dots) and by the fixed ionospheric shell height (black dots) in 2014 for stations in Region II.

277

278 Table 2 presents the quantitative statistical results of average ΔDCB in 2014. For
279 all the stations in each region, the mean values and the root mean squares (RMS) by
280 the optimal ionospheric shell height model are smaller than by the fixed ionospheric
281 height. For Region I, the improvements of TABV are the most significant. Their mean
282 values are reduced to 0.12 and 0.08 TECu, respectively; the root mean squares are
283 reduced by 4.43 and 4.33 TECu, respectively. For Region II, the improvement for
284 DCB estimation are the most obvious for WTZZ, with mean value of ΔDCB decreases
285 from 2.34 to 0.02. We could note that TABV and WTZZ station are quite close to the
286 reference stations in each region.

287

288 **Table 2** Statistical results of mean (ΔDCB) in 2014

Station	Average ΔDCB (TECu) Optimal Ionospheric Height		Average ΔDCB (TECu) Fixed Ionospheric Height	
	Mean	RMS	Mean	RMS
GOLD	0.12	1.82	5.96	6.25
TABV	0.08	2.04	6.06	6.37
QUIN	-1.60	2.31	3.91	4.19
PIE1	-1.38	2.50	4.46	4.84
AMC2	-2.12	2.75	3.09	3.53
PTBB	-0.28	1.23	1.82	2.26
POTS	-0.27	1.00	1.84	2.18
WSRT	-0.41	1.14	1.65	2.10
WTZA	0.09	1.20	2.38	2.73

WTZS	0.14	0.99	2.48	2.76
WTZZ	0.02	1.14	2.34	2.65
GOPE	-0.17	1.00	2.12	2.41
BRUX	-0.42	1.12	1.86	2.13
ONSA	-0.88	1.40	1.10	1.63
ZIMJ	0.48	1.17	2.87	3.13
SPT0	-0.84	1.40	1.14	1.67
OPMT	-0.29	1.21	1.93	2.35
HERS	-0.37	1.19	1.84	2.19
IENG	1.05	1.57	3.44	3.69
VILL	0.59	1.67	3.30	3.66
MADR	0.66	1.71	3.50	3.86

Figure 6 and Figure 7 present the relation between the statistical results of average ΔDCB and the distance to reference stations in each region. The left and the right panels in each figure show the relation of the absolute mean value and the root mean square with the distance to GOLD and PTBB, respectively. For all of the stations, the optimal ionospheric shell height model improves the accuracies of DCB estimation compared to the fixed ionospheric shell height in a statistical sense; both of the absolute mean values and the root mean squares become smaller. For the optimal ionospheric shell height model, the absolute mean values present a positive correlation with the distance to reference station GOLD and PTBB in each region, as well as the root mean squares. By using the linear regression, for Region I, the absolute mean value increases at a rate of about 1.84 TECu per 1000 km and start at

about 0.05 TECu. The RMS value increases at a rate of about 0.75 TECu per 1000 km and starts at about 1.87 TECu. According to the fitting results, the absolute mean value and the RMS less than 1 TECu and 2.25 TECu in the region around GOLD with a radius of 500 km, and less than 2 TECu and 2.62 TECu for the region with a radius of 1000 km. For Region II, the absolute mean value increases at a rate of about 0.30 TECu per 1000 km and start at about 0.25 TECu. The RMS value increases at a rate of about 0.41 TECu per 1000 km and starts at about 1.01 TECu. According to the fitting results, the absolute mean value and the RMS less than about 0.40 TECu and 1.21 TECu in the region around PTBB with a radius of 500 km, and less than about 0.55 TECu and 1.42 TECu for the region with a radius of 1000 km. For the two regions, the RMSs presents stronger linear relation with distance comparing to the means.

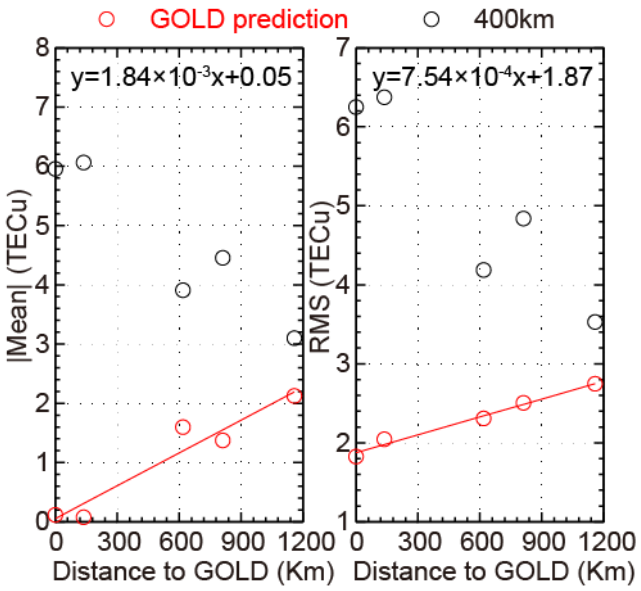

Fig.6 Relation of the accuracy for DCB estimation with the distance to GOLD. The

red lines are the linear fitting results

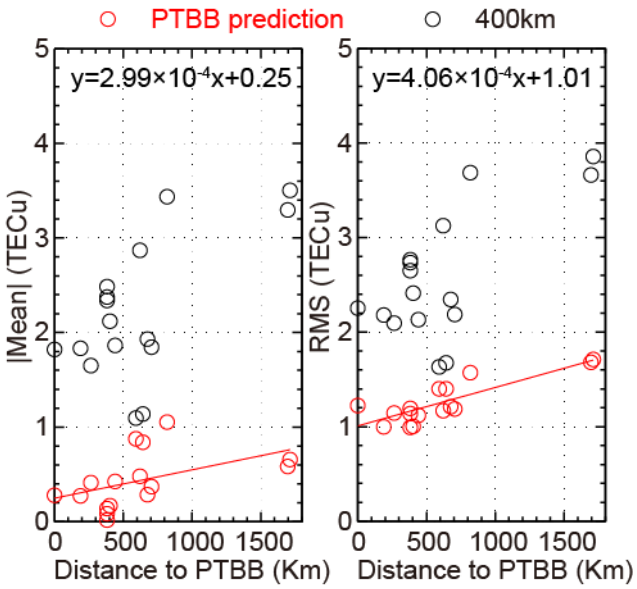

Fig.7 Relation of the accuracy for DCB estimation with the distance to PTBB. The red lines are the linear fitting results

Summary

In this study, we investigate the implementation and validation of optimal ionospheric shell height derived from IGS station to non-IGS station or isolated GNSS receiver. We establish two optimal ionospheric shell height models by the 40th-order of Fourier series based on the data of IGS station GOLD and PTBB in two separate regions These two models are applied to the stations in each region, where the distance to GLOD ranges from 136.67 to 1159.09 km and the distance to PTBB ranges from

190.82 to 1712.27 km. The main findings are summarized as follows:

1) The optimal ionospheric shell height model improves the accuracy of DCB estimation comparing to the fixed shell height for all of the stations in a statistical sense. This results indicate the feasibility of applying the optimal ionospheric shell height derived from IGS station to other neighboring stations. The IGS station can calculate and predict the daily optimal ionospheric shell height, and then release this value to the nearby non-IGS stations or isolated GNSS receivers.

2) For other station in each region, the error of DCB by the optimal ionospheric shell height increases linearly with the distance to the reference GOLD and PTBB station. For the mean and the RMS of the daily average ΔDCBs, in region I, the slopes are about 1.84 and 0.75 TECu per 1000 km; in region II, the slopes are about 0.30 and 0.41 TECu per 1000 km. This results indicate the horizontal spatial correlation of regional ionospheric electron density distribution. For different region, the error at 0 km (i.e. the error for the reference station) is different, which should be also considered.

As the requirement of this experiment, we just analyze two regions in mid-latitude due to the insufficiency of long-term P1 data. We also ignore the orientation of isolated GPS receivers to the reference station.

Acknowledgments

This study is based on data services provided by the IGS (International GNSS Service) and CODE (the Center for Orbit Determination in Europe). This work is supported by the National Natural Science Foundation of China (NSFC grant 41574146 and 41774162).

Reference

Birch MJ, Hargreaves JK, Bailey GJ (2002) On the use of an effective ionospheric height in electron content measurement by GPS reception. Radio Sci 37(1):1015. https://doi.org/10.1029/2000RS002601

Brunini C, Camilion E, Azpilicueta F (2011) Simulation study of the influence of the ionospheric layer height in the thin layer ionospheric model. J Geod 85(9):637–645. https://doi.org/10.1007/s00190-011-0470-2

Clynch JR, Coco DS, Coker CE (1989) A versatile GPS ionospheric monitor: high latitude measurements of TEC and scintillation. In: Proceedings of ION GPS-89, the 2nd International Technical Meeting of the Satellite Division of The Institute of Navigation, Colorado Springs, CO, 22–27 September 1989, pp 445-450

Horvath I, Crozier S (2007) Software developed for obtaining GPS-derived total electron content values. Radio Sci 42(2):RS2002

Huang Z, Yuan H (2014) Ionospheric single-station TEC short-term forecast using RBF neural network. Radio Sci 49(4):283–292

Jiang H, Wang Z, An J, Liu J, Wang N, Li H (2018) GPS Solut. https://doi.org/10.1007/s10291-017-0671-0

Klobuchar A (1987) Ionospheric time-delay algorithm for single-frequency GPS users. IEEE Trans Aerosp Electron Syst AES-23(3):325–331

Lanyi GE, Roth T (1988) A comparison of mapped and measured total ionospheric electron content using Global Positioning System and beacon satellite observations. Radio Sci 23(4):483–492

Li M, Yuan Y, Zhang B, Wang N, Li Z, Liu X, Zhang X (2017) Determination of the optimized single-layer ionospheric height for electron content measurements over China. Journal of Geodesy. https://doi.org/10.1007/s00190-017-1054-6

Lomb NR (1976) Least-squares frequency analysis of unequally spaced data. Astrophysics and space science 39(2):447-462

Lu W, Ma G, Wang X, Wan Q, Li J (2017) Evaluation of ionospheric height assumption for single station GPS-TEC derivation. Advances in Space Research 60(2):286-294

Mannucci AJ, Wilson BD, Yuan DN, Ho CH, Lindqwister UJ, Runge TF (1998) A global mapping technique for GPS-derived ionospheric total electron content measurements. Radio Sci 33(3):565–583

Nava B, Radicella SM, Leitinger R, Coïsson P (2007) Use of total electron content data to analyze ionosphere electron density gradients. Adv Space Res 39(8):1292–1297

Rideout W, Coster A (2006) Automated GPS processing for global total electron content data. GPS Solut 10:219–228. https://doi.org/10.1007/S10291-006-0029-5

Sardón E, Rius A, Zarraoa N (1994) Estimation of the transmitter and receiver differential biases and the ionospheric total electron content from global positioning system observations. Radio Science 29(3):577–586

Scargle JD (1982) Studies in astronomical time series analysis. II-Statistical aspects of spectral analysis of unevenly spaced data. The Astrophysical Journal 263:835-853

Schaer S (1999) Mapping and predicting the earth's ionosphere using the global positioning system. Ph.D. dissertation, Astronomical Institute, University of Bern, Bern, Switzerland

Smith DA, Araujo-Pradere EA, Minter C, Fuller-Rowell T (2008) A comprehensive evaluation of the errors inherent in the use of a two-dimensional shell for modeling the ionosphere. Radio Sci 43:RS6008. doi: 10.1029/2007RS003769

Sovers OJ, Fanselow JL (1987) Observation model and parameter partials for the JPL VLBI parameter estimation software MASTERFIT-1987. NASA STI/Recon Technical Report N, vol 88

Wang XL, Wan QT, Ma GY, Li JH, Fan JT (2016) The influence of ionospheric thin shell height on TEC retrieval from GPS observation. Res Astron Astrophys 16(7):016

Warnant R (1997) Reliability of the TEC computed using GPS measurements—the problem of hardware biases. Acta Geodaetica et Geophysica Hungarica 32(3–4):451–459. https://doi.org/10.1007/BF03325514

Wild U (1994) Ionosphere and satellite systems: permanent GPS tracking data for modelling and monitoring. Geodätisch-geophysikalische Arbeiten in der Schweiz, Band 48

Zhao J, Zhou C (2018) On the Optimal Height of Ionospheric Shell for Single-Site TEC Estimation. GPS Solut. https://doi.org/10.1007/s10291-018-0715-0

420 Zus F, Deng Z, Heise S, Wickert J (2017) Ionospheric mapping functions based on
421 electron density fields. GPS Solut. https://doi.org/10.1007/s10291-016-0574-5

422

423 **Author Biographies**

Jiaqi Zhao is a Ph.D. student at School of Electronic Information, Wuhan University in Wuhan, China. His current research focuses on ionospheric TEC modeling, the analysis of ionospheric thin layer, ionospheric refraction correction based on GNSS and ionospheric three-dimensional tomographic inversion.

Chen Zhou is an associate professor at School of Electronic Information, Wuhan University in Wuhan, China. He mainly focuses on the research of ionospheric physics, geospace modeling, and geospace detection.